Therapeutics, Targets, and Chemical Biology

Cancer Research

AZD8055 Is a Potent, Selective, and Orally Bioavailable ATP-Competitive Mammalian Target of Rapamycin Kinase Inhibitor with *In vitro* and *In vivo* Antitumor Activity

Christine M. Chresta[1], Barry R. Davies[1], Ian Hickson[2], Tom Harding[1], Sabina Cosulich[1], Susan E. Critchlow[1], John P. Vincent[1], Rebecca Ellston[1], Darren Jones[1], Patrizia Sini[1], Dominic James[1], Zoe Howard[1], Phillippa Dudley[1], Gareth Hughes[1], Lisa Smith[2], Sharon Maguire[2], Marc Hummersone[2], Karine Malagu[2], Keith Menear[2], Richard Jenkins[1], Matt Jacobsen[1], Graeme C.M. Smith[1], Sylvie Guichard[1], and Martin Pass[1]

Abstract

The mammalian target of rapamycin (mTOR) kinase forms two multiprotein complexes, mTORC1 and mTORC2, which regulate cell growth, cell survival, and autophagy. Allosteric inhibitors of mTORC1, such as rapamycin, have been extensively used to study tumor cell growth, proliferation, and autophagy but have shown only limited clinical utility. Here, we describe AZD8055, a novel ATP-competitive inhibitor of mTOR kinase activity, with an IC_{50} of 0.8 nmol/L. AZD8055 showed excellent selectivity (~1,000-fold) against all class I phosphatidylinositol 3-kinase (PI3K) isoforms and other members of the PI3K-like kinase family. Furthermore, there was no significant activity against a panel of 260 kinases at concentrations up to 10 μmol/L. AZD8055 inhibits the phosphorylation of mTORC1 substrates p70S6K and 4E-BP1 as well as phosphorylation of the mTORC2 substrate AKT and downstream proteins. The rapamycin-resistant T37/46 phosphorylation sites on 4E-BP1 were fully inhibited by AZD8055, resulting in significant inhibition of cap-dependent translation. *In vitro*, AZD8055 potently inhibits proliferation and induces autophagy in H838 and A549 cells. *In vivo*, AZD8055 induces a dose-dependent pharmacodynamic effect on phosphorylated S6 and phosphorylated AKT at plasma concentrations leading to tumor growth inhibition. Notably, AZD8055 results in significant growth inhibition and/or regression in xenografts, representing a broad range of human tumor types. AZD8055 is currently in phase I clinical trials. *Cancer Res; 70(1); 288–98. ©2010 AACR.*

Introduction

The mammalian target of rapamycin (mTOR) is a serine/threonine kinase belonging to the phosphatidylinositol 3-kinase (PI3K)–like kinase (PIKK) superfamily of kinases. It functions as a sensor of mitogen, energy, and nutrient levels and is a central controller of cell growth and a negative regulator of autophagy (1, 2). Mitogenic signals are transmitted to mTOR via PI3K and AKT (3, 4). mTOR kinase forms two distinct multiprotein complexes called mTORC1 (containing Raptor and PRAS40) and mTORC2 (containing Rictor and Protor). mTORC1, the molecular target of rapamycin, phosphorylates downstream proteins p70S6K (S6K) and 4E-BP1, both involved in protein translation (5). mTORC2 phosphorylates AKT on Ser^{473}, increasing its enzymatic activity by ~5- to 10-fold (6, 7). In normal physiology, mTOR activity is tightly regulated: Phosphorylation of S6K by mTOR induces the degradation of IRS1, decreasing insulin-driven AKT activity and, therefore, mTOR activity (8, 9). The activity of mTOR is also regulated by the energy sensor AMP-activated protein kinase, which stabilizes the TSC1/TSC2 complex and decreases mTOR activity (10). In cancers, increased signaling through mTOR can be due to enhanced upstream signaling through activating mutations in receptor tyrosine kinases or PI3K, or through loss-of-function mutations in PTEN or LKB1, all of which are associated with an increase in phosphorylated AKT (pAKT; ref. 11).

mTORC1 controls essential functions in cells, such as protein translation, cell growth, and autophagy. Rapamycin is an allosteric inhibitor of mTORC1 that does not directly affect mTORC2, except in a small subset of cell lines where, after prolonged exposure, it decreases mTORC2 function by decreasing mTOR protein levels (7). Perhaps surprisingly, considering its major effect on cell growth and autophagy in yeast, rapamycin has limited effect on overall protein synthesis, induces only partial growth inhibition, and is a poor inducer of autophagy in cancer cell lines (5, 12). Recent reports using ATP-competitive inhibitors of mTOR kinase suggest that allosteric inhibition of mTORC1 by rapamycin does not recapitulate inhibition of mTOR kinase activity (13–15). In particular, a decrease in phosphorylation of 4E-BP1 at

Authors' Affiliations: [1]AstraZeneca, Cheshire, United Kingdom and [2]KuDOS Pharmaceuticals Ltd., Cambridge, United Kingdom

Note: Supplementary data for this article are available at Cancer Research Online (http://cancerres.aacrjournals.org/).

C.M. Chresta and B.R. Davies contributed equally to this work.

Corresponding Author: Christine M. Chresta, AstraZeneca, Alderley Park, Macclesfield, Cheshire SK10 4TG, United Kingdom. Phone: 44-1625-517862; Fax: 44-1625-519749; E-mail: Christine.Chresta@astrazeneca.com.

doi: 10.1158/0008-5472.CAN-09-1751

position 37 and 46 is observed with mTOR kinase inhibitors but not with rapamycin (14). This leads to a greater inhibition of cap-dependent translation compared with rapamycin. Additionally, inhibition of mTORC1 by rapamycin and analogues results in the release of the negative feedback loop between S6K and IRS1, leading to hyperactivation of AKT (16). In contrast, mTOR kinase inhibitors inhibit AKT phosphorylation. Rapamycin and analogues have only shown clinical activity as a single agent in a limited number of tumor types (renal cancer and mantle cell lymphoma; ref. 17). Cloughesy and colleagues (18) showed that in PTEN-deficient patients with glioblastoma, hyperactivation of AKT after rapamycin treatment was associated with shorter time to progression, suggesting that the absence of AKT inhibition through mTORC2 targeting limited antitumor activity.

Historically, several molecules inhibiting both PI3K and mTOR, such as LY294002 or PI-103, have been used as "probe compounds" to investigate the biology of the PI3K pathway. Novel agents with dual PI3K and mTOR pharmacology, such as NVP-BEZ235 and XL-765, are now in clinical development in oncology (19). More recently, *in vitro* data have been reported for the ATP-competitive small-molecule inhibitors of mTOR kinase activity PP242 or Torin1. However, no antitumor activity or tumor pharmacodynamic effects were reported (13–15). Herein, we described the preclinical pharmacology of AZD8055, a first-in-class orally available, potent, and specific inhibitor of mTOR kinase activity with profound growth-inhibitory effect *in vitro* and antitumor activity *in vivo*. AZD8055 is currently in phase I clinical development.

Materials and Methods

Chemicals. (5-{2,4-Bis[(3*S*)-3-methylmorpholin-4-yl]pyrido [2,3-*d*]pyrimidin-7-yl}-2-methoxyphenyl)methanol (AZD8055; Fig. 1*A*) was identified through screening of a small library of compounds based around a pyridopyrimidine scaffold (to be described elsewhere). For *in vitro* studies, AZD8055 was prepared as 10 mmol/L stock solution in DMSO and stored under nitrogen. For studies in mice, AZD8055 was dissolved in captisol (CyDex) and diluted to a final captisol concentration of 30% (w/v). AZD8055 was administered by oral gavage (0.1 mL/10 g of body weight) once or twice daily.

Antibodies. All antibodies were obtained from Cell Signaling Technology, except phosphorylated PRAS40 (pPRAS40) T246 (Biosource) and NDRG1 (total) and phosphorylated NDRG1 (pNDRG1; Dario R. Alessi, University of Dundee).

Cell culture. Cell lines were cultured as monolayers in RPMI 1640 supplemented with 10% (v/v) FCS and 2 mmol/L L-glutamine.

Purified enzyme assays. Inhibition of mTOR was evaluated using two methodologies: The high-throughput assay used an α screen capture complex technology (Perkin-Elmer) with a recombinant truncated FLAG-tagged mTOR (amino acids 1362–2549; expressed in HEK293 cells) and a biotinylated p70 peptide substrate. In addition, native mTOR activity was assayed using immunoprecipitation of full-length mTOR from HeLa cytoplasmic extract, and the endogenous mTOR is in protein complexes with Rictor and Raptor. A kinase

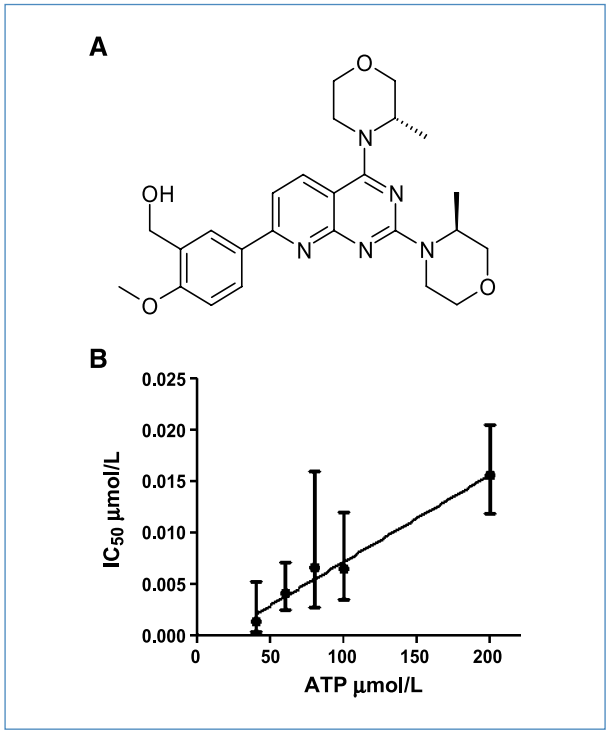

Figure 1. AZD8055 is an ATP-competitive mTOR kinase inhibitor. *A*, chemical structure of AZD8055. *B*, IC_{50}s of AZD8055 are plotted against the concentration of ATP in the enzymatic assay.

assay was performed in the presence of recombinant 4E-BP1 protein as substrate with detection of the phosphorylated product through an ELISA format. The activity of the lipid kinases, class I PI3Ks α, β, δ, and γ, was measured using recombinant PI3Ks with the lipid PIP2 as substrate. Assays for the ataxia-telangiectasia mutated (ATM) and DNA-dependent protein kinase (DNA-PK) were performed as described previously (20). Finally, counterscreen against 260 kinases was carried out at a fixed concentration of 10 μmol/L AZD8055 (Millipore, Inc.).

Kinetic analysis. The activity of mTOR was assayed using the recombinant mTOR technique described above. For inhibition experiments, AZD8055 was added to the reaction mixture and preincubated for 10 min before addition of ATP. Inhibition was performed at 1 to 3,000 nmol/L of AZD8055 in varying concentrations of ATP (40–200 μmol/L).

Cell-based determinations of mTOR inhibition. A high-throughput screening cell-based assay was developed using MDA-MB-468 cells to detect mTORC1 and mTORC2 activity. Cells were exposed for 2 h to increasing concentrations of AZD8055 or rapamycin. At the end of the incubation period, cells were fixed, washed, and probed with antibodies against S473 pAKT or against S235/236 phosphorylated S6 (pS6). Levels of phosphorylation were assessed using an Acumen laser scanning cytometer (TTP Labtech).

Immunoblotting. Cells were lysed on ice with buffer containing 150 mmol/L NaCl, 1 mmol/L EGTA, 1 mmol/L EDTA, 1% Triton X-100, 50 mmol/L NaF, 20 mmol/L Tris-HCl (pH 7.6), 0.1% SDS, protease, and phosphatase inhibitors. Total

protein (20–40 μg) was separated on a 12% Bis-Tris Novex gel and analyzed by immunoblotting. Membranes were blocked in 5% nonfat milk in 1× TBS/0.1% Tween 20 and then probed with the respective primary antibodies overnight at 4°C. After washing and incubation with secondary antibodies, the immunoblotted proteins were visualized using the horseradish peroxidase SuperSignal West Dura Chemiluminescence Substrate according to the manufacturer's instructions.

Inhibition of cap-dependent translation. HEK293 cells were stably transfected with a bicistronic reporter cloned at AstraZeneca with the *Renilla* luciferase gene under the control of a viral internal ribosome entry site (IRES) and the firefly luciferase gene under the control of cap-dependent translation. Cells were treated for 6 h with compounds in medium containing 10% FCS; luciferase activity was then measured using a Dual-Luciferase kit (Promega).

Growth inhibition and autophagy analysis. For growth inhibition and acridine staining, cells were exposed to increasing concentrations of AZD8055 for 72 to 96 h and stained for cell nuclei (0.03 mg/mL Hoechst 33342) and acidic vesicles (1 μg/mL acridine orange). Images were captured at 450 and 536 nm on an ArrayScan II (Cellomics) platform, and the percentage of acidic vesicles and the number of cells were quantified. For LC3 assessment, cells were exposed to e64d/pepstatin (10 μg/mL) for 30 to 90 min before incubation with AZD8055. Cells were lysed on ice and analyzed by immunoblotting.

In vivo *studies.* Specific, pathogen-free, female nude mice (*nu/nu:Alpk*) were housed and maintained in specific, pathogen-free conditions. The facilities have been approved by the Home Office and meet all current regulations and standards of the United Kingdom. The mice were used between the ages of 8 and 12 wk in accordance with institutional guidelines, and all procedures were carried out under United Kingdom Home Office Project Licence 30/2934.

Tumor cells (10^6 for U87-MG, 5×10^6 for A549) were injected s.c. in a volume of 0.1 mL, and mice were randomized into control and treatment groups when tumor size reached 0.2 cm^3. AZD8055 was formulated in 30% (w/v) captisol (pH 3.0). The control group received the vehicle only. Tumor volumes (measured by caliper), animal body weight, and tumor condition were recorded twice weekly for the duration of the study. The tumor volume was calculated (taking length to be the longest diameter across the tumor and width to be the corresponding perpendicular diameter) using the following formula: (length × width) × $\sqrt{}$(length × width) × (π/6).

For pharmacodynamic studies, animals were randomized when tumor size reached 0.5 cm^3. The treatment groups received a single dose of AZD8055 and the control group received vehicle only. Tumor samples and blood were collected at various times after drug administration. The expression of pAKT and pS6 was determined in xenograft tissue by immunoblotting as described above. Ki67 nuclear staining was carried out using formalin-fixed, paraffin-embedded A549 xenografts. Ki67 immunohistochemical nuclear staining was scored using an algorithm developed for scoring percentage positive nuclei on an ACIS II image analyzer (ChromaVision Medical Systems, Inc.) using standard threshold settings.

Plasma pharmacokinetic analysis. Plasma samples were extracted by protein precipitation in acetonitrile. Following centrifugation, the supernatants were mixed with water in a ratio of 1 in 5 (volume for volume). Extracts were analyzed by high-performance liquid chromatography/mass spectrometry using a reversed-phase Synergi Hydro-RP column (Phenomenex) and a gradient mobile phase containing water/acetonitrile/formic acid. Peaks were detected using a Micromass ZQ2000 mass spectrometer. The assay had a range of 0.02 to 17 μg/mL.

Statistical analysis. *In vivo* studies: Growth inhibition from the start of treatment was assessed by comparison of the differences in tumor volume between control and treated groups. Because the variance in mean tumor volume data increases proportionally with volume (and is therefore disproportionate between groups), data were log transformed to remove any size dependency before statistical evaluation. Statistical significance was evaluated using a one-tailed, two-sample *t* test.

Results

***AZD8055 is a selective ATP-competitive inhibitor of mTOR kinase* in vitro.** AZD8055 was identified through screening of a small library of compounds based around a pyridopyrimidine scaffold (Fig. 1*A*). The inhibitory activity of AZD8055 against mTOR was evaluated using two different assays. Using the truncated recombinant mTOR enzyme, the IC_{50} for AZD8055 was 0.13 ± 0.05 nmol/L. Using native mTOR enzyme complexes extracted from HeLa cells, the IC_{50} was 0.8 ± 0.2 nmol/L (Supplementary Table S1). Homology models and structure-activity relationship data suggest that AZD8055 binds to the ATP binding cleft of mTOR kinase in an analogous manner to that seen for LY294002 in PI3Kγ (21). Enzymatic reactions carried out using 40 to 200 μmol/L of ATP resulted in a linear increase in the IC_{50}, indicating that AZD8055 binds competitively with ATP (Fig. 1*B*). The K_i for AZD8055 was identified to be 1.3 nmol/L. AZD8055 was counterscreened against the most closely related kinases, class I and class III PI3K lipid kinases and the PIKK family members ATM and DNA-PK, where it exhibited at least a 1,000-fold differential in potency (Supplementary Table S1). Finally, AZD8055 showed no significant activity against a commercially available panel of 260 kinases at 10 μmol/L (data not shown).

AZD8055 inhibits mTORC1 and mTORC2 and prevents feedback to AKT. Cellular active mTOR compounds were detected using a high-throughput immunocytochemical screening assay in MDA-MB-468 cells. Phosphorylation of AKT was measured at Ser^{473} (mTORC2 substrate) and phosphorylation of ribosomal protein S6 was measured at $Ser^{235/236}$ (indirect substrate of mTORC1). The direct substrate of mTORC1, p70S6K, was not used for the immunocytochemical assay due to detection of nonspecific proteins by the antibody. However, immunoblotting indicates that inhibition of phosphorylation of $Ser^{235/236}$ on ribosomal S6 protein occurs with a similar dose dependency to inhibition of Thr^{389} on p70S6K in MDA-MB-468 cells (Fig. 2*A, inset*). The cellular IC_{50}s for

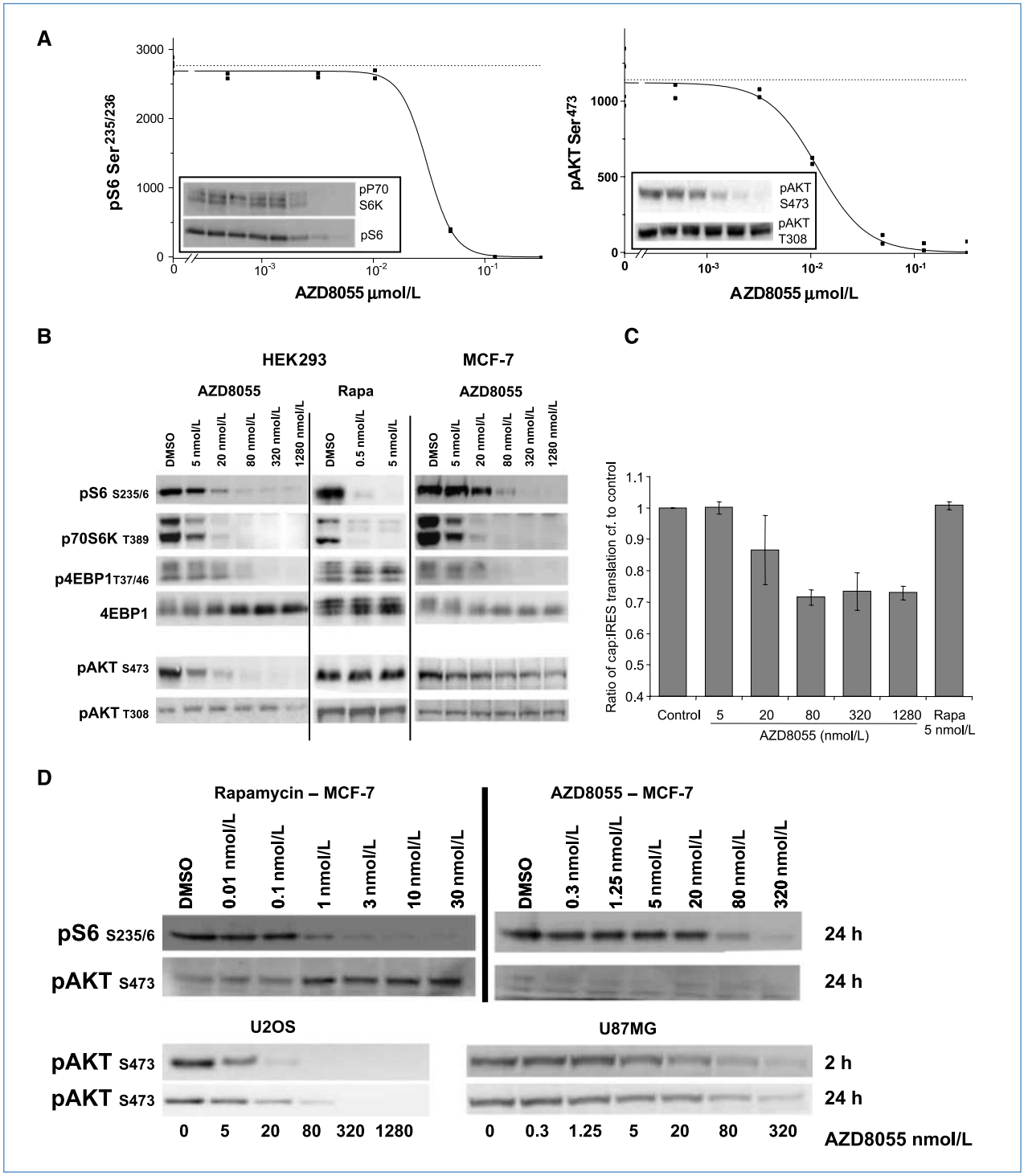

Figure 2. AZD8055 inhibits rapamycin-resistant functions of mTORC1, and the simultaneous inhibition of mTORC1 and mTORC2 prevents feedback to AKT Ser^{473}. *A,* inhibition of pS6 at Ser$^{235/236}$ (mTORC1) and pAKT at Ser^{473} (mTORC2) detected by a high-throughput immunocytochemistry assay in MDA-MB-468 cells in the presence of increasing concentrations of AZD8055 for 2 h. *Insets,* representative immunoblots of MDA-MB-468 whole-cell lysates treated with AZD8055 at 0 to 1,280 nmol/L. *B,* inhibition of mTORC1 and mTORC2 substrates in HEK293 and MCF-7 cells, exposed for 2 h to increasing concentrations of AZD8055 or rapamycin (*Rapa*; HEK293), determined by immunoblotting of whole-cell lysates with the indicated antibodies. *C,* inhibition of translation in HEK293 cells stably transfected with a bicistronic reporter vector. Cells were treated for 6 h with compound (in medium containing 10% FCS), and the ratio of firefly (cap dependent) to *Renilla* (IRES dependent) luciferase activity was then measured in three experiments. Data are relative to the ratio in untreated cells. *D, top,* pAKT and pS6 in MCF-7 after 24-h treatment with AZD8055 or rapamycin; *bottom*, pAKT in U2OS and U87MG cells after 2- or 24-h treatment with AZD8055.

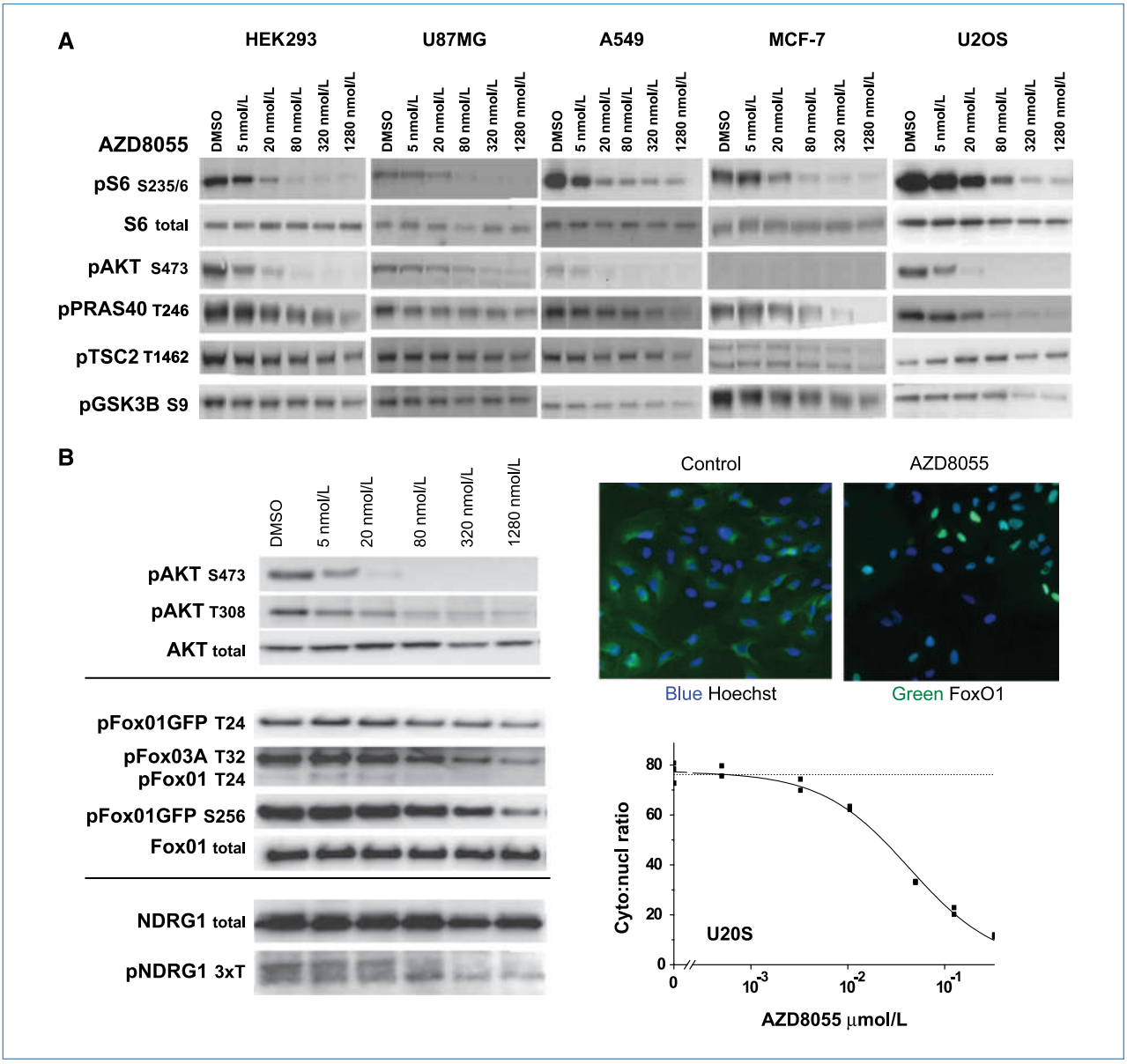

Figure 3. AZD8055 inhibits mTORC2 downstream signaling. *A,* the phosphorylation of PRAS40, GSK3β, and TSC2 on AKT-dependent phosphorylation sites was determined by immunoblotting in HEK293, U87-MG, A549, MCF-7, and U2OS cell lines in the presence of increasing concentrations of AZD8055 after 2 h of exposure. *B,* inhibition of the phosphorylation of AKT, FoxO1GFP, FoxO1, and FoxO3a and the SGK substrate NDRG1 in U2OS cells treated for 2 h with AZD8055 measured by immunoblotting (*left*), and nuclear accumulation of FoxO1GFP assessed in U2OS cells exposed to increasing concentrations of AZD8055 for 2 h (*right*). Representative pictures of cellular localization of FoxO1 in U2OS cells exposed to vehicle or 1 μmol/L AZD8055.

AZD8055 were calculated as 24 ± 9 nmol/L (n = 13) for pAKT Ser^{473} and 27 ± 3 nmol/L (n = 12) for pS6 $Ser^{235/236}$ (Fig. 2*A*). Pulse chase experiments indicated that the activity of AZD8055 was readily reversible following compound removal, with pS6 levels returning to control levels 15 minutes after drug removal (data not shown).

Inhibition of mTORC1 substrates was then investigated in more detail in other cell types and compared with rapamycin. p70S6K, its substrate ribosomal protein S6, and 4E-BP1 $Thr^{37/46}$ (Fig. 2*B*) were all inhibited in a concentration-dependent manner; 5 nmol/L AZD8055 resulted in 70% to 80% inhibition of p70S6K in MCF-7 and HEK cells. Rapamycin, in contrast, potently inhibited p70S6K but did not result in inhibition of 4E-BP1 phosphorylation on $Thr^{37/46}$ (Fig. 2*B*). The effect of inhibition of 4E-BP1 phosphorylation on translation was assessed in HEK293 cells stably transfected with a bicistronic reporter with the firefly luciferase gene under the control of cap-dependent translation and the *Renilla* luciferase under control of an IRES. AZD8055 resulted in inhibition of cap-dependent translation at concentrations closely

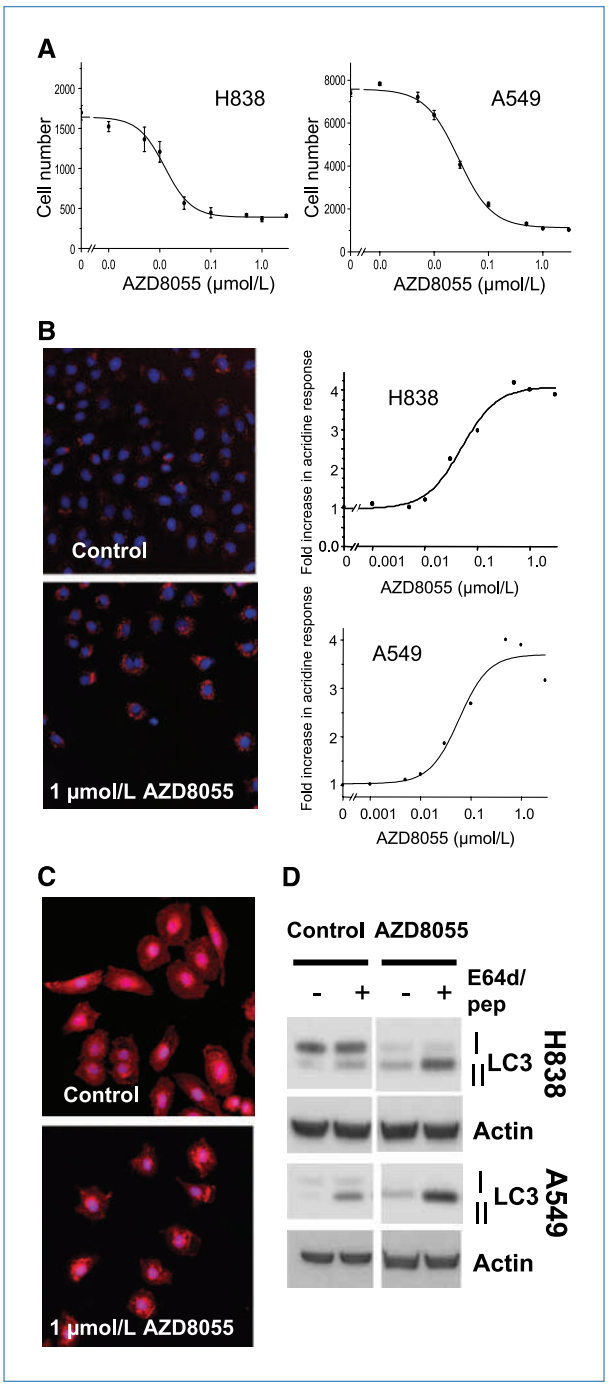

Figure 4. AZD8055 inhibits cellular proliferation and induces autophagy. *A*, decrease in cell number determined by nuclear staining in H838 and A549 exposed to increasing concentrations (0–3 μmol/L) for 72 h. *B*, intensity of acridine staining in H838 and A549 cells exposed to increasing concentrations of AZD8055 (0–3 μmol/L) for 72 h. Representative pictures of H838 exposed to vehicle or 1 μmol/L AZD8055. *C*, increase of LC3 processing in H838 cells determined by immunofluorescence after exposure to 1 μmol/L AZD8055 for 48 h. *D*, expression of LC3 (LC3-I and LC3-II) determined by immunoblotting in cell extracts from H838 and A549 cells exposed to 1 μmol/L AZD8055 for 48 h in the presence or absence of E64d and pepstatin.

mirroring those resulting in inhibition of phosphorylated 4E-BP1 (p4E-BP1) Thr$^{37/46}$ (Fig. 2*C*). In contrast, rapamycin did not affect translation, consistent with lack of inhibition of 4E-BP1 phosphorylation.

In all cell types, AZD8055 inhibited phosphorylation of AKT on Ser^{473} more potently and completely than on Thr^{308} [Figs. 2*A* (*inset*) and *B* and 3*B*], indicating that AZD8055 inhibits mTORC2 but does not directly affect PDK1; this is consistent with other mTOR inhibitors and genetic mTORC2 knockout (13, 15, 22). Simultaneous inhibition of mTORC1 and mTORC2 by AZD8055 prevented feedback to AKT Ser^{473}. There was no evidence of induction of pAKT Ser^{473} by AZD8055 at either 2 hours (Figs. 2*B* and 3*A*) or 24 hours (Fig. 2*D*) in MCF-7 and all other cell lines studied. In contrast, treatment of MCF-7 cells for 24 hours with rapamycin resulted in a significant increase in the phosphorylation of AKT on Ser^{473} (Fig. 2*D*), consistent with the release of the negative feedback loop between S6K and IRS1 previously reported (16, 23). We conclude that AZD8055 inhibits mTOR kinase activity in cells, which results in a more complete inhibition of mTORC1 than with rapamycin, and the inhibition of mTORC2 prevents phosphorylation of AKT through the IRS1 feedback loop.

Effect of AZD8055 on mTORC2 downstream signaling. Genetic knockout of mTORC2 impairs both AKT and SGK function (15, 22). In the case of AKT, it predominantly affects the phosphorylation of the AKT substrate FoxO but not the AKT substrates PRAS40, TSC2, and GSK3β (22). The effect of AZD8055 on AKT substrates was evaluated in cell lines with a range of genetic alterations: HEK293, U87-MG (PTEN null), A549 (Kras and LKB1 mutant), MCF-7 (PIK3CA mutant, p70S6K amplified), and U2OS (PTEN null). In all cell types, AZD8055 induced a concentration-dependent decrease of pPRAS40 T246 with a maximum inhibition of 70% to 95% depending of the cell line (Fig. 3*A*). Inhibition of phosphorylation of pTSC2 on T1462 and GSK3β on S9 was detected to varying levels, and in some cell lines, inhibition of GSK3β on S9 was relatively weak (e.g., inhibition reached <30% in U87MG cells). The effect of AZD8055 on FoxO was assessed in U2OS cells engineered to express FoxO1GFP (BioImage). AZD8055 decreased the phosphorylation of exogenous FoxO1GFP on T24 and S256 and endogenous FoxO1 T24 (very weak bands) and FoxO3a T32 in a dose-dependent manner, resulting in a concentration-dependent relocalization of FoxO1GFP from the cytoplasm to the nucleus (Fig. 3*B*). The drug concentration leading to a nuclei-to-cytoplasm ratio of 50% was 67 ± 26 nmol/L (n = 3).

The effect of AZD8055 on SGK activity was evaluated using the SGK substrate NDRG1 because endogenous SGK is not readily detectable by Western blotting (15). NDRG1 phosphorylation is inhibited in Rictor- and Sin1-null mouse embryo fibroblasts (MEF) and has been reported to be a useful surrogate for SGK activity and a marker of mTORC2 function (15). AZD8055 results in a concentration-dependent decrease in pNDRG1 in U2OS cells (Fig. 3*B*).

***AZD8055 induces growth inhibition and autophagy* in vitro.** mTOR is an important factor involved in control of cell growth and autophagy in both *Saccharomyces*

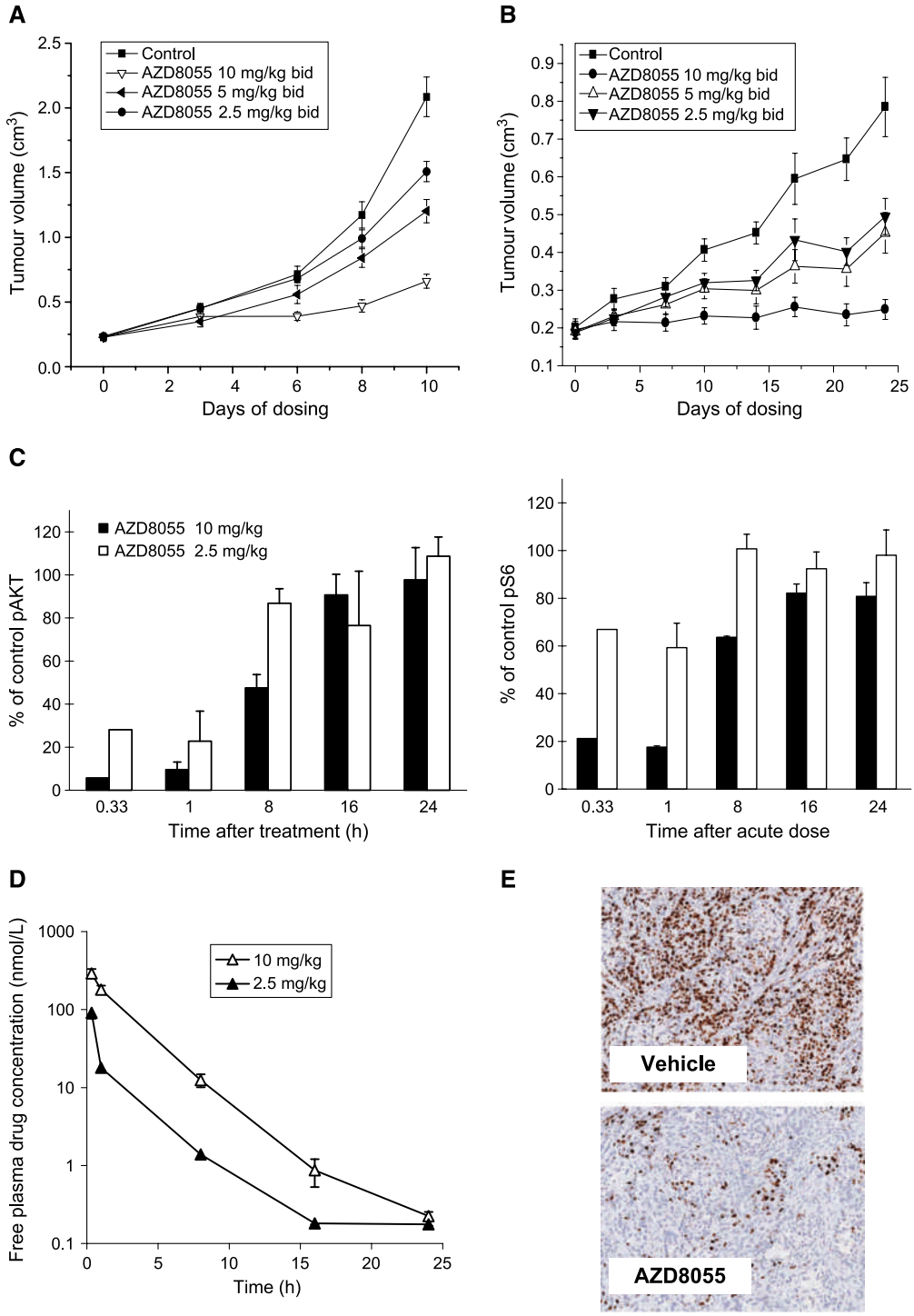

Figure 5. AZD8055 induces a dose-dependent tumor growth inhibition and pharmacodynamic effect in tumor xenografts. Mice bearing U87-MG xenografts (*A*) or A549 xenografts (*B*) were treated with AZD8055 at 2.5, 5, and 10 mg/kg twice daily (*bid*) by oral gavage. Tumor volumes are plotted against time. *C* to *E,* mice bearing U87-MG xenografts were treated with a single dose of 2.5 mg/kg (*white columns*) or 10 mg/kg of AZD8055 (*black columns*). *C,* plasma and xenografts tumors were collected 20 min and 1, 8, 16, and 24 h after drug administration, and the pharmacodynamic effect on pAKT (*left*) and pS6 (*right*) was measured by immunoblotting. *D,* pharmacokinetics of AZD8055 after administration of 2.5 and 10 mg/kg of AZD8055. Plasma-free drug concentrations are plotted against time after drug administration. *E,* Ki67 nuclear staining determined by immunohistochemistry in A549 xenografts collected after four daily administrations of 10 mg/kg AZD8055 (4 h after the final dose).

cerevisiae and mammalian cells (12). Interestingly, rapamycin has shown some discrepancy between inhibition of the pathway, inhibition of cell growth, and induction of autophagy in mammalian cells (24). This might be due to its limited effect on mTORC1 (partial inhibition of p4E-BP1) and its lack of effect on mTORC2. The effect of AZD8055 on cellular proliferation was measured in H838 and A549 [both non–small cell lung cancer (NSCLC) cell lines] and U87MG (glioblastoma; data not shown) determined by nuclear staining after 72 h of exposure to increasing concentrations of AZD8055 (Fig. 4*A*). Drug concentrations inducing 50% inhibition of proliferation were 53 ± 13 nmol/L in U87MG and 50 ± 9 nmol/L and 20 ± 10 nmol/L in A549 and H838, respectively.

Rapamycin has been shown to induce autophagy; hence, we evaluated whether AZD8055 would affect this process. The effect of AZD8055 on autophagosome formation in H838 and A549 cells was first assessed by measuring the formation of punctate acidic vesicles in the cytoplasm detected by acridine orange as an indicator of autophagy (25). A concentration-dependent increase in acridine staining localized to punctate cytoplasmic structures was observed after 72 hours of exposure to AZD8055, suggesting the presence of autophagosomes (Fig. 4*B*). The maximum increase in acridine staining was observed with 1 μmol/L AZD8055. Furthermore, immunostaining with antibodies to light chain 3 (LC3) indicated a concentration-dependent increase in this staining pattern, consistent with LC3 being localized to these acidic vesicles (Fig. 4*C*). Finally, LC3-I is normally converted into LC3-II (LC3-I covalently bound to phosphatidylethanolamine) during autophagosome formation but is converted back to LC3-I by protease cleavage during autophagosome maturation. The overall formation of LC3-II was detected by preincubating cells with E64d/leupeptin, inhibiting protease-induced reconversion of LC3-II into LC3-I. AZD8055 increased LC3-II levels in H838 and A549 cells, and this increase was more pronounced in the presence of E64d/leupeptin, consistent with an increase in autophagosome formation (Fig. 4*D*).

AZD8055 induces significant tumor growth inhibition in a broad range of human tumor xenografts. In mice bearing U87-MG (PTEN null) glioblastoma xenografts, oral treatment with AZD8055 resulted in a dose-dependent tumor growth inhibition of 33%, 48%, and 77% with 2.5, 5, and 10 mg/kg/d twice daily, respectively (Fig. 5*A*). A similar dose dependency was observed in nude mice bearing A549 xenografts: tumor growth inhibition was 44%, 55%, and 93% after 2.5, 5, and 10 mg/kg/d twice daily, respectively (Fig. 5*B*). AZD8055 also resulted in significant inhibition of tumor growth and/or regression in breast, lung, colon, prostate, and uterine xenograft models when administered either twice daily at 10 mg/kg or daily at a dose of 20 mg/kg (Table 1). Consistent with rapalogues, AZD8055 results in a transient modest increase in glucose in mice (data not shown).

AZD8055 induces a pharmacodynamic effect on both pS6 and pAKT in U87-MG and A549 xenografts. The pharmacodynamic effects of AZD8055 were determined in mice bearing U87-MG xenografts after a single oral administration of AZD8055 at either 2.5 or 10 mg/kg. The levels of pAKT (S473; corrected for total glyceraldehyde-3-phosphate dehydrogenase protein) decreased to 5% and 28% of control levels 20 minutes after drug administration of 10 and 2.5 mg/kg of AZD8055, respectively (Fig. 5*C*). The inhibition of pAKT was >50% for at least 8 hours in animals receiving 10 mg/kg AZD8055. A similar pattern was observed for pS6 (S235/236) with levels down to 21% and 67% of control levels 20 minutes after administration of 10 and 2.5 mg/kg AZD8055, respectively (Fig. 5*C*). Phosphorylation of S6 recovered slightly faster than AKT with treated levels being 63% of control levels 8 hours after drug administration. Free concentrations of AZD8055 of 90 and 291 nmol/L were observed 20 minutes after administration of 2.5 and 10 mg/kg, respectively (Fig. 5*D*). The pharmacodynamic activity tracked well with the concentrations of the compound in plasma: A mean-free drug concentration of ~12 nmol/L was sufficient to decrease the phosphorylation of AKT by at least 50% in U87-MG xenografts. This was consistent with a concentration sufficient to inhibit pAKT in U87-MG cells *in vitro* (~10 nmol/L).

The level of proliferation was determined by Ki67 staining in A549 xenografts 4 hours after four daily doses of 20 mg/kg AZD8055. The percentage of positive nuclei decreased from 32 ± 2% in xenografts from animals treated with vehicle only to 10 ± 1% in xenografts from animals treated with 20 mg/kg

Table 1. Antitumor activity *in vivo* induced by AZD8055 administered orally at a dose of 10 mg/kg twice daily or 20 mg/kg daily

Cell line	Tumor type	Dose	Tumor growth inhibition (%)
U87-MG	Glioma	10 mg/kg BID	77
BT-474c	Breast	20 mg/kg QD	99
A549	NSCLC	10 mg/kg BID	93
Calu-3	NSCLC	20 mg/kg QD	125
LoVo	Colon	10 mg/kg BID	69
SW620	Colon	10 mg/kg BID	70
PC3	Prostate	10 mg/kg BID	66
MES-SA	Uterus	20 mg/kg QD	65

Abbreviations: BID, twice daily; QD, daily.

AZD8055 (Fig. 5*E*), confirming the antiproliferative effect of AZD8055 observed *in vitro*.

Discussion

The present study describes AZD8055 as an orally bioavailable, potent, and selective mTOR kinase inhibitor with ~1,000-fold selectivity against PI3K isoforms or related PIKK family members. AZD8055 inhibits tumor cell proliferation *in vitro* and *in vivo*. In some cell lines, it also induces the formation of acidic vesicles, consistent with a process of macroautophagy.

Rapamycin and analogues have proven that mTOR is an attractive target in cancer. The relative limited clinical utility of rapalogues was, until recently, thought to be largely due to the release of the S6K, IRS negative feedback loop, and lack of inhibition of mTORC2 and, therefore, increase in AKT activity. Indeed, Cloughesy and colleagues (18) reported that rapamycin treatment induces an increase in pAKT and the AKT substrate pPRAS40 in a subset of patients with PTEN-deficient glioblastoma. Moreover, increase of pPRAS40 was associated with shorter survival (18). Dual specificity inhibitors, which target the activity of PI3K lipid kinases and mTOR (BEZ235 and XL-765), have entered clinical development (19). These agents inhibit mTORC1 and mTORC2 but also inhibit a broad range of PI3K isoforms. In contrast, AZD8055 potently and selectively inhibits mTOR kinase activity (~1 nmol/L K_i) without inhibiting PI3K. Recently, the *in vitro* biochemical profile of three selective mTOR kinase inhibitors (Torin1, PP242, and Ku-0063794) has been described in model systems, including MEFs, L6 myotubes, and human embryonic kidney cells (13–15). Surprisingly, mTOR kinase inhibitors result in differential effects on both mTORC1 and mTORC2 compared with rapamycin. We have extended these findings to a broad range of human cancer cell models both *in vitro* and *in vivo* in preparation for clinical development of AZD8055 as an anticancer agent.

AZD8055 potently inhibits phosphorylation of AKT on the mTORC2 site, Ser^{473}, in all cell types studied; in addition, the T308 site is also inhibited in some cell types, although not as potently as S473. This is in contrast to genetic knockout of Sin1 or Rictor, where phosphorylation of S473 is ablated but the T308 site remains phosphorylated (22, 26). The inhibition of T308 probably reflects a decrease in the ability of PDK1 to phosphorylate AKT on T308 when S473 phosphorylation is transiently but fully inhibited; similar findings have been reported with PP242 and Ku-0063794 (13, 15). This hypothesis is supported by studies using cells transfected with S473A and S473D mutants of AKT (to mimic phosphorylation of S473), where little or no inhibition of T308 occurs with the selective mTOR kinase inhibitors PP242 (structurally distinct) and Ku-0063794 (structurally similar to AZD8055; refs. 13, 15). The inhibition of AKT phosphorylation induced by AZD8055 was associated with a decrease in phosphorylation of AKT downstream substrates PRAS40, TSC2, GSK3β, and FoxO1/3a. It is interesting to note that AZD8055 resulted in an unequal magnitude of inhibition of these AKT substrates, $pPRAS40^{T246}$ was particularly sensitive in all cell types, whereas $pTSC2^{T1462}$ and $pGSK3\beta^{S9}$ were inhibited more weakly and inhibition varied in a cell type–specific manner. Phosphorylation of FoxO was studied in U2OS cells; phosphorylation of endogenous $pFoxO3a^{T32}$ and $pFoxO1^{T24}$ was inhibited more potently by AZD8055 than $pTSC2^{T1462}$ and $pGSK3\beta^{S9}$, but the differences were not as extreme as seen in genetic knockouts. Previous reports using insulin-stimulated mTORC2-deficient MEFs (Sin1, mLST8, or Rictor null) have described FoxO3 phosphorylation on T32 to be significantly inhibited by loss of mTORC2 function, whereas $pTSC2^{T1462}$ or $pGSK3\beta^{S9}$ remain relatively unaffected (22, 26). Because the AKT substrates PRAS40 and TSC2 control the overall activity of mTORC1 (27), inhibition of mTORC2 activity by AZD8055 is likely to also indirectly affect mTORC1 activity. Further study in this area may be instructive in differentiating mTOR kinase inhibitors from rapamycin and direct inhibitors of AKT kinase.

AZD8055 binds to the mTOR kinase domain and therefore directly affects mTORC1 and has a more profound effect on mTORC1 than rapamycin. Several functions of mTORC1 are indeed controlled by mTOR but are unaffected by rapamycin. One of the main functions of mTORC1 is the control of mRNA translation (5). A recent study showed that 5′TOP mRNA translation is highly dependent on mTOR kinase activity rather than Rictor or Raptor and that rapamycin had limited or no effect on this process (28). mTOR also affects translation by modulating the phosphorylation of S6K on T389 and 4E-BP1 on T37, T46, S65, and T70. The phosphorylation of these sites on S6K and 4E-BP1 is dependent on an interaction with Raptor, indicating they are mTORC1 substrates (29). Surprisingly, although rapamycin induces a sustained inhibition of S6K phosphorylation, it has limited effect on the growth factor–sensitive phosphorylation sites of 4E-BP1 (T37/46) and even hyperphosphorylates 4E-BP1 over time (30). This translates into a modest inhibition of cap-dependent translation. The present study shows that AZD8055 significantly decreases the phosphorylation of 4E-BP1 on the rapamycin-insensitive T37/46 sites and potently inhibits cap-dependent translation at low nanomolar concentrations, consistent with the concentrations that inhibit proliferation. Studies using the mTOR kinase inhibitors PP242, Ku-0063794, and Torin1 have shown the T37/46 site of 4E-BP1 to be independent of mTORC2 because phosphorylation was unaffected by Sin1 and Rictor knockout but dependent on Raptor and because phosphorylation was significantly decreased by Raptor RNA interference (13–15). This suggests that the ATP-competitive inhibitors have differential effects on mTORC1 compared with rapamycin (13–15). The inhibition of phosphorylation on T37/46 has been associated with a greater effect on cap-dependent translation, growth inhibition, and potentially autophagy (5). More recently, eIF4GI was shown to be a major factor linking inhibition of cap-dependent translation and biological effect such as growth inhibition and autophagy (31). Rapamycin affects the growth factor–sensitive phosphorylation sites on eIF4GI (32). In most cell lines studied *in vitro*, rapamycin and analogues induce a partial growth inhibition and limited autophagy (12, 33). Conversely, AZD8055 induces a profound growth

inhibition both *in vitro* and *in vivo*. mTORC1 also controls autophagy directly by phosphorylating Atg1, although Atg1 might exert a negative feedback loop on mTOR. mTOR indirectly regulates autophagy, as the negative feedback loop controlled by S6K may control the basal level of autophagy (34–36). In some cell lines, AZD8055 induces the formation of acidic vesicles associated with LC3, consistent with the induction of autophagosome formation. Inhibition of mTORC1 via inhibition of mTOR kinase is therefore likely to be responsible for the greater induction of autophagy induced by AZD8055 compared with that observed with rapamycin. However, further studies are needed to clarify the effect of AZD8055 on proteins such as Atg1.

In vivo, AZD8055 was well tolerated and induced a dose-dependent growth inhibition and/or regression in a broad range of tumor xenografts. This was associated with a rapid and dose-dependent pharmacodynamic effect on both pS6 and pAKT. To date, the mTOR kinase inhibitors PP242, Ku-0063794, and Torin1 have not reported *in vivo* activity in tumor models (13–15). PP242 induces pharmacodynamic effects in fat, muscle, and liver tissue (13). Further studies are needed to confirm whether a pharmacodynamic effect of PP242 in xenograft tumors is associated with antitumor effect while maintaining a therapeutic index.

In summary, AZD8055 is a potent and selective mTOR kinase inhibitor that acts on both mTORC1 and mTORC2 and downstream substrates. AZD8055 is orally bioavailable and induces a dose-dependent growth inhibition of tumor cell lines both *in vitro* and *in vivo*. AZD8055 is currently being evaluated in phase I studies in a variety of tumors.

Disclosure of Potential Conflicts of Interest

No potential conflicts of interest were disclosed.

Acknowledgments

We thank Sangeetha Palakurthi for cloning the translation reporter construct and Professor Dario Alessi's laboratory for many helpful discussions and for providing the NDRG antibodies.

The costs of publication of this article were defrayed in part by the payment of page charges. This article must therefore be hereby marked *advertisement* in accordance with 18 U.S.C. Section 1734 solely to indicate this fact.

Received 5/13/09; revised 10/15/09; accepted 10/28/09; published OnlineFirst 12/22/09.

References

1. Lindsley JE, Rutter J. Nutrient sensing and metabolic decisions. Comp Biochem Physiol B Biochem Mol Biol 2004;139:543–59.
2. Guertin DA, Sabatini DM. Defining the role of mTOR in cancer. Cancer Cell 2007;12:9–22.
3. Long X, Lin Y, Ortiz-Vega S, Busch S, Avruch J. The Rheb switch 2 segment is critical for signaling to target of rapamycin complex 1. J Biol Chem 2007;282:18542–51.
4. Shaw RJ, Kosmatka M, Bardeesy N, et al. The tumor suppressor LKB1 kinase directly activates AMP-activated kinase and regulates apoptosis in response to energy stress. Proc Natl Acad Sci U S A 2004;101:3329–35.
5. Proud CG. mTORC1 signalling and mRNA translation. Biochem Soc Trans 2009;37:227–31.
6. Sarbassov DD, Guertin DA, Ali SM, Sabatini DM. Phosphorylation and regulation of Akt/PKB by the rictor-mTOR complex. Science 2005;307:1098–101.
7. Sarbassov DD, Ali SM, Sengupta S, et al. Prolonged rapamycin treatment inhibits mTORC2 assembly and Akt/PKB. Mol Cell 2006;22:159–68.
8. Sun XJ, Goldberg JL, Qiao LY, Mitchell JJ. Insulin-induced insulin receptor substrate-1 degradation is mediated by the proteasome degradation pathway. Diabetes 1999;48:1359–64.
9. Shah OJ, Wang Z, Hunter T. Inappropriate activation of the TSC/Rheb/mTOR/S6K cassette induces IRS1/2 depletion, insulin resistance, and cell survival deficiencies. Curr Biol 2004;14:1650–6.
10. Manning BD, Logsdon MN, Lipovsky AI, et al. Feedback inhibition of Akt signaling limits the growth of tumors lacking Tsc2. Genes Dev 2005;19:1773–8.
11. Guertin DA, Sabatini DM. An expanding role for mTOR in cancer. Trends Mol Med 2005;11:353–61.
12. Pattingre S, Espert L, Biard-Piechaczyk M, Codogno P. Regulation of macroautophagy by mTOR and Beclin 1 complexes. Biochimie 2008;90:313–23.
13. Feldman ME, Apsel B, Uotila A, et al. Active-site inhibitors of mTOR target rapamycin-resistant outputs of mTORC1 and mTORC2. PLoS Biol 2009;7:e38.
14. Thoreen CC, Kang SA, Chang JW, et al. An ATP-competitive mammalian target of rapamycin inhibitor reveals rapamycin-resistant functions of mTORC1. J Biol Chem 2009;284:8023–32.
15. Garcia-Martinez JM, Moran J, Clarke RG, et al. Ku-0063794 is a specific inhibitor of the mammalian target of rapamycin (mTOR). Biochem J 2009;421:29–42.
16. O'Reilly KE, Rojo F, She QB, et al. mTOR inhibition induces upstream receptor tyrosine kinase signaling and activates Akt. Cancer Res 2006;66:1500–8.
17. Faivre S, Kroemer G, Raymond E. Current development of mTOR inhibitors as anticancer agents. Nat Rev Drug Discov 2006;5:671–88.
18. Cloughesy TF, Yoshimoto K, Nghiemphu P, et al. Antitumor activity of rapamycin in a phase I trial for patients with recurrent PTEN-deficient glioblastoma. PLoS Med 2008;5:e8.
19. Maira SM, Stauffer F, Brueggen J, et al. Identification and characterization of NVP-BEZ235, a new orally available dual phosphatidylinositol 3-kinase/mammalian target of rapamycin inhibitor with potent *in vivo* antitumor activity. Mol Cancer Ther 2008;7:1851–63.
20. Hickson I, Zhao Y, Richardson CJ, et al. Identification and characterization of a novel and specific inhibitor of the ataxia-telangiectasia mutated kinase ATM. Cancer Res 2004;64:9152–9.
21. Walker EH, Pacold ME, Perisic O, et al. Structural determinants of phosphoinositide 3-kinase inhibition by wortmannin, LY294002, quercetin, myricetin, and staurosporine. Mol Cell 2000;6:909–19.
22. Guertin DA, Stevens DM, Thoreen CC, et al. Ablation in mice of the mTORC components raptor, rictor, or mLST8 reveals that mTORC2 is required for signaling to Akt-FOXO and PKCα, but not S6K1. Dev Cell 2006;11:859–71.
23. Sun SY, Rosenberg LM, Wang X, et al. Activation of Akt and eIF4E survival pathways by rapamycin-mediated mammalian target of rapamycin inhibition. Cancer Res 2005;65:7052–8.
24. Takeuchi H, Kondo Y, Fujiwara K, et al. Synergistic augmentation of rapamycin-induced autophagy in malignant glioma cells by phosphatidylinositol 3-kinase/protein kinase B inhibitors. Cancer Res 2005;65:3336–46.
25. Kanzawa T, Kondo Y, Ito H, Kondo S, Germano I. Induction of autophagic cell death in malignant glioma cells by arsenic trioxide. Cancer Res 2003;63:2103–8.

26. Jacinto E, Facchinetti V, Liu D, et al. SIN1/MIP1 maintains rictor-mTOR complex integrity and regulates Akt phosphorylation and substrate specificity. Cell 2006;127:125–37.
27. Sancak Y, Thoreen CC, Peterson TR, et al. PRAS40 is an insulin-regulated inhibitor of the mTORC1 protein kinase. Mol Cell 2007; 25:903–15.
28. Patursky-Polischuk I, Stolovich-Rain M, Hausner-Hanochi M, et al. The TSC-mTOR pathway mediates translational activation of TOP mRNAs by insulin largely in a raptor- or rictor-independent manner. Mol Cell Biol 2009;29:640–9.
29. Beugnet A, Tee AR, Taylor PM, Proud CG. Regulation of targets of mTOR (mammalian target of rapamycin) signalling by intracellular amino acid availability. Biochem J 2003;372:555–66.
30. Choo AY, Yoon SO, Kim SG, Roux PP, Blenis J. Rapamycin differentially inhibits S6Ks and 4E-BP1 to mediate cell-type-specific repression of mRNA translation. Proc Natl Acad Sci U S A 2008;105: 17414–9.
31. Ramirez-Valle F, Braunstein S, Zavadil J, Formenti SC, Schneider RJ. eIF4GI links nutrient sensing by mTOR to cell proliferation and inhibition of autophagy. J Cell Biol 2008;181:293–307.
32. Raught B, Gingras AC, Gygi SP, et al. Serum-stimulated, rapamycin-sensitive phosphorylation sites in the eukaryotic translation initiation factor 4GI. EMBO J 2000;19:434–44.
33. Kim KW, Mutter RW, Cao C, et al. Autophagy for cancer therapy through inhibition of pro-apoptotic proteins and mammalian target of rapamycin signaling. J Biol Chem 2006;281:36883–90.
34. Chang YY, Juhasz G, Goraksha-Hicks P, et al. Nutrient-dependent regulation of autophagy through the target of rapamycin pathway. Biochem Soc Trans 2009;37:232–6.
35. Neufeld TP. Contribution of Atg1-dependent autophagy to TOR-mediated cell growth and survival. Autophagy 2007;3:477–9.
36. Jung CH, Jun CB, Ro SH, et al. ULK-Atg13-FIP200 complexes mediate mTOR signaling to the autophagy machinery. Mol Biol Cell 2009;20:1992–2003.